

# High-susceptibility nanoparticles for micro-inductor core materials

Mathias Zambach<sup>1</sup> , Miriam Varón<sup>1</sup> , Matti Knaapila<sup>2</sup> , Ziwei Ouyang<sup>3</sup> , Marco Beleggia<sup>4,5</sup> , and Cathrine Frandsen<sup>1</sup> \*

<sup>1</sup>DTU Physics, Technical University of Denmark, 2800 Kgs. Lyngby, Denmark

<sup>2</sup>Department of Physics, Norwegian University of Science and Technology, 7491 Trondheim, Norway

<sup>3</sup>DTU Electro, Technical University of Denmark, 2800 Kgs. Lyngby, Denmark

<sup>4</sup>Department of Physics, University of Modena and Reggio Emilia, 41125 Modena, Italy and

<sup>5</sup>DTU Nanolab, Technical University of Denmark, 2800 Kgs. Lyngby, Denmark

(Dated: February 6, 2024)

According to the laws of magnetism, the shape of magnetically soft objects limits the effective susceptibility. For example, spherical soft magnets cannot display an effective susceptibility larger than 3. Although true for macroscopic multi-domain magnetic materials, we show that magnetic nanoparticles in a single-domain state do not suffer from this limitation. This is a consequence of the particle moment being forced to saturation by the predominance of exchange forces, and only allowed to rotate coherently in response to thermal and/or applied fields. We apply statistical mechanics to determine the static and dynamic susceptibility of single-domain particles as a function of size, temperature and material parameters. Our calculations reveal that spherical single-domain particles with large saturation magnetisation and small magneto-crystalline anisotropy, e.g. FeNi particles, can have very a large susceptibility of 200 or more. We further show that susceptibility and losses can be tuned by particle easy axis alignment with the applied field in case of uniaxial anisotropy, but not for particles with cubic anisotropy. Our model is validated experimentally by comparison with measurements on nanocomposites containing spherical  $11 \pm 3$  nm  $\gamma$ -Fe<sub>2</sub>O<sub>3</sub> particles up to 45 vol% finely dispersed in a polymer matrix. In agreement with the calculations for this specific material, the measured susceptibility of the composites is up to 17 ( $\gg 3$ ) and depends linearly on the volume fraction of particles. Based on these results, we predict that nanocomposites of 30 vol% of superparamagnetic FeNi particles in an insulating non-magnetic matrix can have a sufficiently large susceptibility to be used as micro-inductor core materials in the MHz frequency range, while maintaining losses below state-of-the-art ferrites.

## I. INTRODUCTION

Magnetic components, such as inductors and transformers, are essential for power control in many handheld devices. However, realisation of efficient micro-inductors is challenging as miniaturisation suppresses induction [1, 2]. While a decrease in induction can be counteracted by larger susceptibilities and higher operating frequencies, magnetic materials available today become inefficient and heat up rapidly at elevated frequencies due to eddy-current losses [3, 4]. Miniaturisation and increase in efficiency of magnetic components in electronics is therefore limited by soft magnetic material performance [5].

For a magnetic material to be used as a core for micro-inductors, its susceptibility needs to be above 50-100, while losses should remain below 200 mW/cm<sup>3</sup> at an operating frequency of 2 MHz and a flux density of 30 mT [3]. If losses are reduced below 20 mW/cm<sup>3</sup>, a susceptibility range of 20-50 would be acceptable [1, 5].

In conventional magnetic core materials eddy-current losses are minimised by use of composite cores. Here magnetic particles are electrically isolated by a non-conductive matrix. Commercial composite cores often use  $\mu$ m-sized magnetic particles which have particle susceptibilities,  $\chi_p$ , of several thousand, close to the bulk

value. However, these particles are multi-domain in nature and their susceptibility is limited by demagnetisation: The effective susceptibility of the particle,  $\chi_{p,\text{eff}}$ , is

$$\chi_{p,\text{eff}} = \frac{\chi_p}{1 + N\chi_p} = \frac{1}{\frac{1}{\chi_p} + N}, \quad (1)$$

where  $N$  is the demagnetisation factor of the particle along the applied field direction. The effective susceptibility of  $\mu$ m particles is therefore at most  $1/N$ , or 3 in case of spheres where  $N = 1/3$ . Consequently, large effective susceptibilities can only be achieved with particles elongated and aligned along the applied field direction.

Magnetic composites using smaller spherical single-domain magnetic particles have recently emerged [6–12]. It is unclear from the literature if single-domain particles may possess effective susceptibilities above  $1/N$ . Typically, dilute particle systems with relatively low effective susceptibilities have been reported for these type of composites. However, susceptibility measurements on dense systems of single-domain iron nanoparticles indicate that spherical single-domain particles may not be limited by demagnetisation effects in the same way as multi-domain soft spherical magnets [13] although not discussed in the reference.

In order to evaluate particles for use in high-susceptibility nanocomposites, we here set up a framework for calculating the DC- and AC-susceptibility of single-domain magnetic nanoparticles. We focus on pos-

\* fraca@fysik.dtu.dk

sible demagnetisation effects in magnetic particles and derive the susceptibility of blocked and superparamagnetic single-domain particles considering both uniaxial or cubic anisotropy. Our results show that an effective susceptibility above 3 is possible for spherical single-domain magnetic particles. We verify this result by experimental susceptibility measurements on spherical, well-dispersed  $11 \pm 3$  nm  $\gamma\text{-Fe}_2\text{O}_3$  (maghemite) particles in polymer matrix for which we report nanocomposite susceptibilities of up to 17. This experimentally confirms that the susceptibility of single-domain magnetic particles is not limited by demagnetisation effects in the same way as multi-domain particles are. On this basis we predict that nanocomposites containing about 30 vol% FeNi particles with diameters of 15-20 nm could be competitive with state-of-the-art ferrite inductor core materials.

## II. THEORETICAL FRAMEWORK

We consider a stationary single-domain ferromagnetic particle embedded in a solid non-magnetic matrix. For single-domain particles, atom spins align ferromagnetically and rotate coherently such that the magnetic moment of the particle is  $\mathbf{m} = VM_s$ , where  $V$  is the particle volume and  $M_s$  its saturation magnetization. Relevant coordinate systems for below energy consideration are shown in Fig. 1.

### A. Energy considerations

#### 1. Uniaxial anisotropy

Choosing the polar axis to coincide with the uniaxial anisotropy easy axis, as illustrated in Fig. 1a, the anisotropy energy is

$$E_{\text{ua}} = K_u V \sin^2 \theta_m, \quad (2)$$

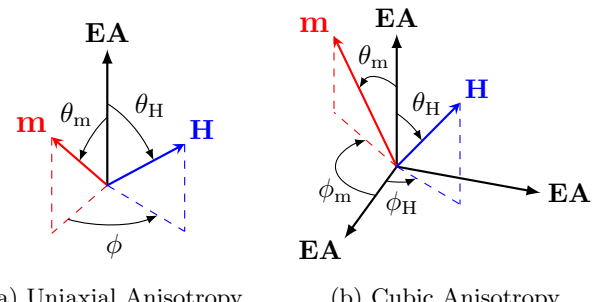
where  $K_u$  is the uniaxial anisotropy constant for the material, and  $\theta_m$  is the angle between the magnetisation and the easy axis of magnetisation, i.e. the polar angle of the magnetisation. The Zeeman energy is

$$E_Z = -\mu_0 m H (\cos \theta_m \cos \theta_H + \sin \theta_m \sin \theta_H \cos \phi), \quad (3)$$

where  $\theta_H$  is the polar angle of the applied field,  $H$  is the applied field amplitude, and  $\phi = \phi_H - \phi_m$  is difference between the azimuth angles of the applied field and the magnetisation.

#### 2. Cubic anisotropy

In case of cubic anisotropy we orient the coordinate system based on the case where the cubic anisotropy constant is positive,  $K_c > 0$ , i.e., 3 mutually orthogonal easy axes, see Fig. 1b. One easy axis is set to the polar



(a) Uniaxial Anisotropy (b) Cubic Anisotropy

Figure 1: Illustration of used coordinate systems and definitions of angles. EA refers to easy axis,  $\mathbf{m}$  is the particle moment, and  $\mathbf{H}$  is the applied field. (a) Uniaxial anisotropy. (b) Cubic anisotropy with easy axes shown for  $K_c > 0$ .

axis and the other two easy axes are along the direction where the azimuth is 0 and  $\pi/2$ . The anisotropy energy can then be expressed as

$$E_c = K_c V \sin^2 \theta_m (\cos^2 \theta_m + \sin^2 \theta_m \sin^2 \phi_m \cos^2 \phi_m), \quad (4)$$

where  $K_c$  is the cubic anisotropy constant. The Zeeman energy for the cubic case is

$$E_Z = -\mu_0 m H \begin{bmatrix} \sin \theta_m \cos \phi_m \\ \sin \theta_m \sin \phi_m \\ \cos \theta_m \end{bmatrix} \cdot \begin{bmatrix} \sin \theta_H \cos \phi_H \\ \sin \theta_H \sin \phi_H \\ \cos \theta_H \end{bmatrix}. \quad (5)$$

### 3. Demagnetisation

The demagnetisation energy of a uniformly magnetised single-domain spheroid particle can be written on the form of a uniaxial anisotropy energy due to the fact that the magnetization of a single-domain particle is always saturated. Thus one obtains the demagnetisation energy

$$E_{H_d} = -\frac{\mu_0}{2} \int_V \mathbf{M}_s \cdot \mathbf{H}_d dV = K_{\text{sh}} V \sin^2 \Theta, \quad (6)$$

with the shape anisotropy constant  $K_{\text{sh}} = \mu_0 M_s^2 (N_{ii} - N_{jj})/2 = K_d (N_{ii} - N_{jj})$ . Here  $N_{ii}$  and  $N_{jj}$  are the demagnetisation factors along the principal spheroid axes.  $K_{\text{sh}}$  is positive (negative) for oblate (prolate) spheroids, respectively, and  $\Theta$  is the angle between the magnetic moment and the longer (shorter) principal spheroid axis. In agreement with [14], we find that if the length difference between the axes is larger than 5-10%, then shape anisotropy dominates over magneto-crystalline anisotropy for most soft magnetic particle materials.

In the next section we derive the effective particle susceptibility, first for single-domain particles vs. that of multi-domain particles, and then for the two limiting single-domain cases: blocked particles and superparamagnetic particles.

## B. Particle susceptibility

### 1. Single-domain versus multi-domain particles

We note that the demagnetisation field in single-domain particles differs from the multi-domain case: The magnitude of the demagnetisation field in single-domain particles does not increase due to an induced magnetisation with applied field as found for multi-domain particles. Instead, the demagnetisation field rotates with the saturated magnetisation according to the demagnetisation factors. This modifies the way that demagnetisation factors enter the effective susceptibility for single-domain particles compared to the case of multi-domain particles as we show below.

The particle susceptibility tensor components,  $\chi_{p_{ij}}$ , and effective particle susceptibility,  $\chi_{p,\text{eff}}$ , for both single-domain and multi-domain particles, can be written as

$$\chi_{p_{ij}} = \frac{\partial M_i}{\partial H_{ij}} \quad \text{and} \quad \chi_{p,\text{eff}} = \frac{\partial(\mathbf{M} \cdot \hat{\mathbf{H}})}{\partial H}. \quad (7)$$

Here,  $M_i$  is the component of the magnetisation in the  $i$ -direction,  $H_{ij}$  is the internal field strength of the particle in the  $j$  direction,  $H$  is the applied field amplitude, and  $\hat{\mathbf{H}}$  is the normalised applied field direction. For uniformly magnetised particles, the demagnetisation field can be described by the demagnetisation tensor components,  $N_{jk}$ , such that the internal field component becomes

$$H_{ij} = H_j + H_{d_j} = H_j - N_{jk}M_k. \quad (8)$$

Starting with the multi-domain case, we assume the linear relationship  $M_j = \chi_p H_{ij}$ . Thus, one finds that  $\chi_{p_{ij}} = (\delta_{ij}/\chi_p + N_{ij})^{-1}$ , such that the effective susceptibility for multi-domain particles is

$$\chi_{p,\text{eff}} = \frac{h_x^2}{N_{xx} + 1/\chi_p} + \frac{h_y^2}{N_{yy} + 1/\chi_p} + \frac{h_z^2}{N_{zz} + 1/\chi_p} \quad (9)$$

with  $h_{x,y,z}$  being the direction cosines of the applied field, i.e.  $\hat{\mathbf{H}} = (h_x, h_y, h_z)$ . This expression is usually known in the format of Eq. (1), where  $N$  is the demagnetisation factor in the applied field direction. Thus, the effective particle susceptibility of a spherical multi-domain particle will be limited to  $\chi_{p,\text{eff}} \leq 3$ .

In case of a single-domain (blocked) particle, the magnetic moment will, without applied field, be aligned to the easy axis (shape and/or crystal). We set the z-axis along this direction such that with zero applied field  $\hat{\mathbf{M}} = \hat{\mathbf{z}}$ . The shape anisotropy energy for a uniformly magnetised ellipsoid is

$$\frac{E}{K_d V} = (N_{xx}m_x^2 + N_{yy}m_y^2 + N_{zz}m_z^2) - \mathcal{H}(\hat{\mathbf{M}} \cdot \hat{\mathbf{H}}), \quad (10)$$

with  $m_{x,y,z}$  being the directional cosines of the magnetisation, i.e.  $\hat{\mathbf{M}} = (m_x, m_y, m_z)$ , and  $\mathcal{H} = 2H/M_s$ . In

absence of an applied field, Eq. (10) can be set equal to the contribution from the magnetisation along the z-axis, i.e.  $E/(K_d V) = N_{zz}$ . Using that  $m_z \approx 1$  for small fields, we can write

$$0 = (N_{xx} - N_{zz})m_x^2 + (N_{yy} - N_{zz})m_y^2 - 2\mathcal{H}(m_xh_x + m_yh_y + h_z). \quad (11)$$

From (11) one can find the x and y components of the magnetisation by setting the energy gradients with respect to  $m_x$  and  $m_y$  to zero, obtaining

$$m_x = \frac{\mathcal{H}h_x}{N_{xx} - N_{zz}} \quad \text{and} \quad m_y = \frac{\mathcal{H}h_y}{N_y - N_{zz}}. \quad (12)$$

The effective susceptibility for a blocked, single-domain particle when considering shape anisotropy is then

$$\chi_{p,\text{eff}} = \frac{h_x^2}{N_{xx} - N_{zz}} + \frac{h_y^2}{N_{yy} - N_{zz}}. \quad (13)$$

This shows that the effective susceptibility depends on the *difference* in demagnetisation factors along the principal axes of the given shape. Thus, we find for single-domain particles that the shape anisotropy does not limit the effective susceptibility to  $1/N$  as for the multi-domain case. In detail, Eq. (13) makes it clear that for spherical single-domain particles, where  $N_{xx} = N_{yy} = N_{zz} = 1/3$ ,  $\chi_{p,\text{eff}}$  is not limited to 3 as in the multi-domain case. Moreover, Eq. (13) establishes that for ellipsoidal particles, the susceptibility will only be limited by  $1/(N_{ii} - N_{jj})$ , which has no upper limit. It is noticeable from Eq. (13) that for single-domain particles (in clear contrast to the multi-domain case) a higher susceptibility is obtained for (near-)spherical particles.

### 2. Thermal effects

For sufficiently small single-domain particles, thermal energy can induce superparamagnetism, i.e. moment fluctuations. The characteristic timescale,  $\tau$ , for relaxation between easy directions, depends on the anisotropy barrier over the thermal energy  $K_u V/(k_B T)$ . Magnetic particles can be classified as blocked or superparamagnetic, depending on how the superparamagnetic relaxation compares to the experimental timescale.

#### i. Blocked particles

For blocked particles, thermal fluctuations are slower than the experimental timescale. In case of uniaxial anisotropy the susceptibility depends on the direction of the applied field with respect to the particle easy axis, cf. the Stoner-Wohlfarth model [15]. For randomly oriented particles, the averaged particle susceptibility [16] is

$$\langle \chi_B \rangle = \langle \cos^2 \theta_H \rangle \chi_B(0) + \langle \sin^2 \theta_H \rangle \chi_B(\pi/2) = \frac{2}{3} \kappa \quad (14)$$

where  $\kappa = K_d/K_u$ , since  $\langle \cos^2 \theta_H \rangle = 1/3$ ,  $\langle \sin^2 \theta_H \rangle = 2/3$ ,  $\chi_B(0) = 0$ , and  $\chi_B(\pi/2) = \kappa$ . Blocked particles with uniaxial anisotropy and easy axis aligned parallel with the applied field will have a square hysteresis loop with coercive field of  $H_c = \kappa M_s$ . For the perpendicularly aligned case, no hysteresis is observed.

Including demagnetisation energy in the Stoner-Wohlfarth model shows, that for spherical particles, where demagnetisation energy is constant, there is no difference in magnetisation or susceptibility. This is due to the fact that a constant energy offset does not change the location of the local energy minimum, and hence does not dictate the direction of the magnetic moment. For non-spherical particles, instead, an effective uniaxial shape anisotropy exists. This will result in competing anisotropies in the particle leading to the concept of effective field. The presence and combination of several uniaxial anisotropies may cause hysteresis loop opening for several directions as in the cubic case [17]. Once again, this does not limit the susceptibility to  $1/N$  as the same arguments as in section II B 1.

For blocked particles with cubic anisotropy, hysteresis loop opening is always observed no matter the direction of the applied field with respect to the 3 or 4 easy axes and thus only a small low field susceptibility is expected [17–19], but it is not limited to  $1/N$ .

### ii. Superparamagnetic particles

Superparamagnetic particles are characterized by thermal fluctuations acting faster than the experimental timescale set by the measurement apparatus. The magnetisation and susceptibility can be found as for a paramagnetic ion. The partition function for a particle can be written as

$$Z = \int_{\Omega} \exp \left[ -\frac{E_i}{k_B T} \right] d\Omega, \quad (15)$$

where the integral over  $\Omega$  indicates integration over all possible energy states  $E_i$ . The relevant single particle energies presented in Eqs. (2)–(6) depend on moment direction, thus the integral in Eq. (15) should here be taken over all possible moment directions:  $\int_{\Omega} d\Omega = \int_0^{2\pi} \int_0^{\pi} \sin \theta_m d\theta_m d\phi_m$ . For shorter notation we define following energy ratios

$$\epsilon_k = \frac{K_u V}{k_B T}, \quad \epsilon_H = \frac{\mu_0 V M_s H}{k_B T}, \quad \epsilon_M = \frac{\mu_0 V M_s^2}{k_B T}. \quad (16)$$

The unit-less component of the mean magnetic moment of a superparamagnetic particle along the direction of the applied field,  $\langle m_{\text{spm}} \rangle$ , can now be found as

$$\langle m_{\text{spm}} \rangle = \frac{1}{Z} \frac{\partial Z}{\partial \epsilon_H}. \quad (17)$$

The mean magnetisation along the direction of the applied field is then  $\langle M_{\text{spm}} \rangle = M_s \langle m_{\text{spm}} \rangle$ . The susceptibil-

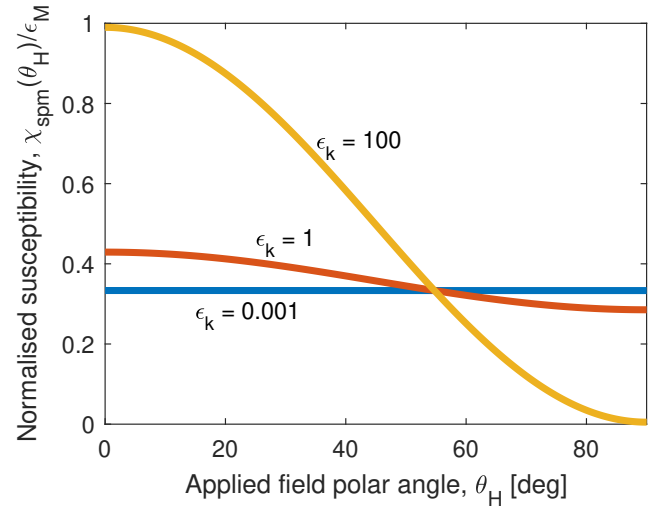


Figure 2: Superparamagnetic particle susceptibility normalised by  $\epsilon_M$  as function of the angle between applied field and uniaxial anisotropy easy axis,  $\theta_M$ , for particles with varying anisotropy barrier  $\epsilon_k$ . Based on Eqs. (18)–(19).

ity can be found as the derivative of the mean magnetisation wrt. the applied field amplitude.

For a non-interacting, uniaxial anisotropy particle with the applied field at an angle  $\theta_H$  to the anisotropy axis we find the superparamagnetic particle susceptibility  $\chi_{\text{spm}}$  is

$$\chi_{\text{spm}}(\theta_H) = \frac{\epsilon_M}{2} [\sin^2 \theta_H + R'/R (3 \cos^2 \theta_H - 1)] \quad (18)$$

with

$$R' = \int_0^1 x^2 \exp(\epsilon_k x^2) dx \quad \text{and} \quad R = \int_0^1 \exp(\epsilon_k x^2) dx. \quad (19)$$

Figure 2 shows a plot of Eq. (18) for different values of  $\epsilon_k$ . For uniaxial anisotropy particles the susceptibility ranges from  $\epsilon_M$  to 0 in case of large anisotropy ( $\epsilon_k \gg 1$ ) as  $R'/R$  goes towards 1. For low anisotropy ( $\epsilon_k \ll 1$ ) the limit of  $R'/R$  is  $1/3$  and the susceptibility of the uniaxial anisotropy particle goes towards the random case value  $\epsilon_M/3$  for all  $\theta_H$ . Including demagnetisation as in Eq. (6) will act as additional uniaxial anisotropy, since  $K_{\text{sh}}$  is equivalent to  $K_u$ . As such it can enhance or decrease the susceptibility depending on the applied field orientation with respect to the easy axis direction.

For non-interacting, randomly oriented particles, one can average over all possible directions and thus recover the well known per particle susceptibility

$$\langle \chi_{\text{spm}} \rangle = \frac{\epsilon_M}{3} = \frac{\mu_0 V M_s^2}{3 k_B T}. \quad (20)$$

For the susceptibility of non-interacting particles with cubic anisotropy we find no dependence of the applied field direction (i.e.  $\theta_H$  and  $\phi_H$ ). The initial susceptibility for the cubic anisotropy case is always the same

as for the randomly oriented uniaxial anisotropy case in the superparamagnetic regime (Eq. (20)), no matter the strength of the anisotropy axis. This can be explained by the symmetric distribution of energy minima along 3 (or 4) easy axes, which does not change the probability of the moment to point along any specific direction, contrary to the uniaxial case where there is 1 direction (or plane) that is statistically more likely. Demagnetisation for the cubic anisotropy case makes the particle behave as uniaxial with only shape anisotropy and no crystalline anisotropy. Additionally, just like in the blocked particle case, the susceptibility depends on differences in demagnetisation factor along the principal axes of the particle, which further supports our arguments from section II B 1.

### iii. Dynamic particle susceptibility

The dependence of the susceptibility on applied field frequency and the crossover from superparamagnetic towards blocked regime can be expressed by the concept of AC-susceptibility [16, 20]. At small  $\epsilon_H$ , where the anisotropy barrier is not changed by the applied field, the AC-susceptibility for an applied sinusoidal field with angular frequency  $\omega$ ,  $\tilde{\chi}(\omega)$ , can be related to the superparamagnetic particle susceptibility,  $\chi_{\text{spm}}$ , and the superparamagnetic relaxation time,  $\tau$ . The AC susceptibility is thus found by a Debye model of the form

$$\tilde{\chi}(\omega) = \frac{\chi_{\text{spm}}}{1 + i\omega\tau} = \chi'(\omega) + i\chi''(\omega), \quad (21)$$

with in- and out-of-phase components  $\chi'(\omega)$  and  $\chi''(\omega)$  [21].

For uniaxial anisotropy particles  $\tau$  depends on the direction of the applied field wrt. the easy axis [16, 20, 22, 23]. Magnetic moment relaxation time perpendicular to the anisotropy axis,  $\tau_{\perp}$ , is assumed to be short, on the timescale of the attempt time  $\tau_0 \approx 10^{-11} - 10^{-9}$  s [24]. Relaxation time over the anisotropy barrier,  $\tau_{\parallel}$ , i.e. parallel to the anisotropy axis, is slower, and often described by Arrhenius-type expressions. The AC-susceptibility for randomly oriented uniaxial anisotropy particles,  $\langle \tilde{\chi}_{\text{spm}}(\omega) \rangle$ , can thus be expressed by the weighted sum of the AC-susceptibility parallel and perpendicular with the easy axis:

$$\langle \tilde{\chi}_{\text{spm}}(\omega) \rangle = \frac{1}{3} \left[ \frac{\chi_{\text{spm}}(0)}{1 + i\omega\tau_{\parallel}} + 2 \frac{\chi_{\text{spm}}(\pi/2)}{1 + i\omega\tau_{\perp}} \right], \quad (22)$$

with  $\chi_{\text{spm}}(0)$  and  $\chi_{\text{spm}}(\pi/2)$  from Eq. (18). The relaxation times  $\tau_{\parallel}$  and  $\tau_{\perp}$  are found as [22, 23]

$$\tau_{\parallel} = \begin{cases} \tau_0 2R'/(R - R') & \text{for } \epsilon_k \leq 2, \\ \tau_0 \sqrt{\pi} \exp(\epsilon_k)/(2\epsilon_k^{3/2}) & \text{for } \epsilon_k > 2, \end{cases} \quad (23a)$$

$$\tau_{\perp} = \tau_0 2(R - R') / (R + R') \quad \text{for all } \epsilon_k. \quad (23b)$$

From the out-of-phase component one can estimate the hysteresis loss per particle by  $P_H = \omega\mu_0 H^2 \chi''(\omega)/2$  for

small  $H$ . For low anisotropy particles the out-of-phase component of the AC-susceptibility is overestimated by the above and can be regarded as an upper bound [21].

For cubic anisotropy, expressions similar to the parallel case of (23) exist, but with a lower effective anisotropy constant  $K_{\text{eff}}$  of  $K_{\text{eff}} = K_c/4$  for  $K_c > 0$  and  $K_{\text{eff}} = K_c/12$  for  $K_c < 0$  [25–28].

## III. EVALUATION OF PARTICLES FOR NANOCOMPOSITES

The formalism developed so far enables an estimate the maximum susceptibilities of single-domain particles. We consider candidate materials to be used with applied field frequencies up to 10 MHz, and discuss if the resulting effective susceptibilities are sufficient for inductor core applications.

### A. Particle material

Figure 3 displays the derived effective in-phase susceptibility as function of particle diameter from the superparamagnetic regime to the blocked regime for randomly oriented, spherical nanoparticles at 10 MHz. Particle materials are maghemite ( $\gamma\text{-Fe}_2\text{O}_3$ ), Fe, Ni, FeNi, and FeCo. We have used reported effective uniaxial anisotropy constants and saturation magnetisation values for nanoparticles of these materials [29–33]. We note that effective uniaxial anisotropy constants commonly are reported for nanoparticles although the materials themselves are known to have cubic magneto-crystalline anisotropy. We have not considered the dependence of saturation magnetisation and effective anisotropy constant on synthesis routine and particle size, and used values reported for 3–10 nm sized particles (21–50 nm for FeNi).

Fig. 3 shows that superparamagnetic particle susceptibility increases with particle size up to when their relaxation time becomes comparable to the periodicity of the exciting field. As size increases further the susceptibility declines towards the blocked value, which depends on saturation magnetisation and anisotropy, but not on the particle size, cf. Eq. (14). Our results predict that FeCo and FeNi particles reach susceptibilities above 100 in the superparamagnetic region. In literature low values of particle or composite material susceptibility are reported, however, [13] states "particle susceptibility" of 122 for 8 nm diameter Fe particles, which seems to fall in line with the predictions in Fig. 3, but for lower applied field frequency.

We find that nanoparticles with high saturation magnetization and low anisotropy feature the largest susceptibility, as their magnetic moments are larger and their transition to the blocked regime occurs at larger diameters. The superparamagnetic region towards the susceptibility peak is of particular interest for applications due to the potential combination of high-susceptibility

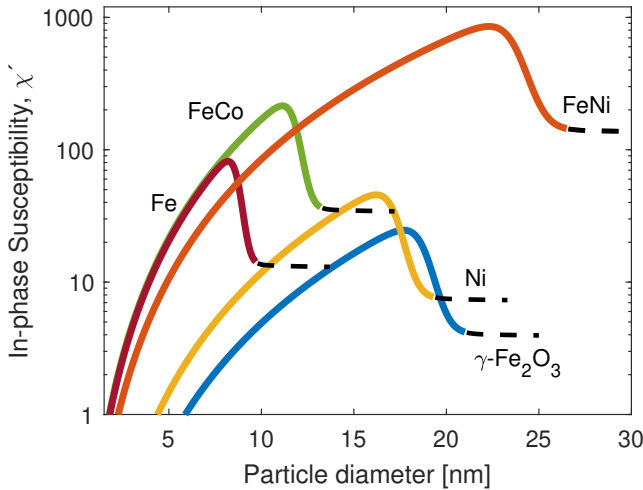


Figure 3: Average per particle in-phase susceptibility for randomly oriented, spherical particles in 10 MHz sinusoidal fields as a function of particle size. Calculations are based on Eqs. (18) and (22)-(23),  $\tau_0 = 10$  ns,  $T = 298$  K, and material parameters; Maghemite ( $\gamma\text{-Fe}_2\text{O}_3$ ):  $K_u = 10$  kJ/m<sup>3</sup>,  $M_s = 303$  kA/m, Ni:  $K_u = 13$  kJ/m<sup>3</sup>,  $M_s = 470$  kA/m, Fe:  $K_u = 100$  kJ/m<sup>3</sup>,  $M_s = 1750$  kA/m, FeCo:  $K_u = 40$  kJ/m<sup>3</sup>,  $M_s = 1790$  kA/m, FeNi:  $K_u = 5$  kJ/m<sup>3</sup>,  $M_s = 1260$  kA/m. Blocked regime indicated by dashed line.

and limited hysteresis loss. We suggest, based on Fig. 3, the use of  $\sim 9$  nm FeCo particles or  $\sim 20$  nm FeNi particles for high-susceptibility applications such as micro-inductor core materials.

The susceptibility of around 130 for the blocked FeNi particles, as seen in Fig. 3, could in principle be of interest, as such susceptibility value may be sufficient for use in micro-inductors. However, use of blocked particles requires particle alignment as only the  $\theta_H = \pi/2$  case will show no hysteresis losses.

### B. Particle Orientation and AC-effects

Equations (22)-(23) show that the dynamic susceptibility depends on the direction of the particle with respect to the applied field. Figure 4 shows this frequency dependence of the in- and out-of-phase susceptibility for uniaxial anisotropy FeNi particles with log-normal distributed diameters of  $20 \pm 1$  nm for cases with anisotropy axes parallel, perpendicularly and randomly oriented wrt. the applied field. It is seen for the frequency range of 10 kHz to 10 MHz that the 20 nm FeNi particles aligned with their easy axis parallel to the applied field have a in-phase susceptibility of 1600, i.e., more than twice the value for the randomly oriented case (700) and more than six times the perpendicular "hard-axis" case (230). At around 100 MHz the in-phase part drops and the out-of-phase com-

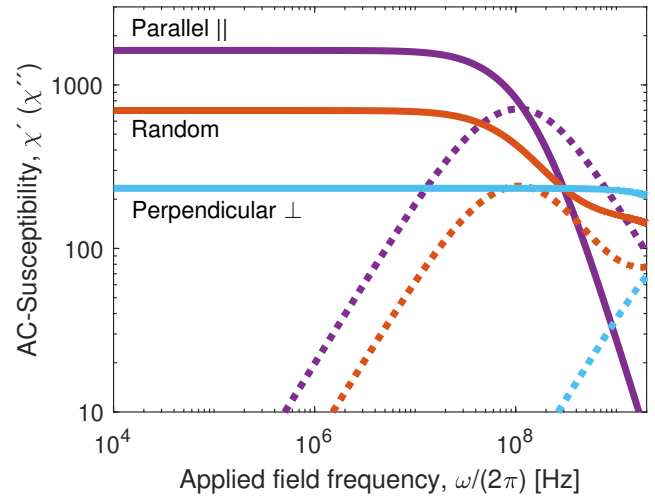


Figure 4: In-phase (solid) and out-of-phase (dashed) susceptibility of  $20 \pm 1$  nm diameter (log-normal distributed) FeNi particles with easy axis oriented randomly, parallel or perpendicular to applied field axis as function of applied field frequency. Calculations are based on (22)-(23),  $\tau_0 = 10$  ns,  $T = 298$  K, effective uniaxial anisotropy of  $K_u = 5$  kJ/m<sup>3</sup> and  $M_s = 1260$  kA/m. Parallel and perpendicular alignment refer to  $\theta_H = 0$  and  $\pi/2$  respectively.

ponent peaks for the parallel aligned and random cases. This is due to the fact that  $\omega \approx 1/\tau_{||}$  in this frequency range. For the random case the susceptibility drops towards the random orientation blocked susceptibility of Eq. (14). For the perpendicular case we observe a completely flat susceptibility up to the GHz regime where  $\omega \approx 1/\tau_{\perp}$ . For the perpendicular case we find that susceptibility does not depend on particle size, with values close to the blocked, aligned case of Eq. (14). Alignment of particles by easy/hard axis thus allows for tuning of the magnetic properties.

### C. Nanocomposite susceptibility

Having established a framework to calculate particle susceptibility we now turn to the topic of nanocomposite susceptibility for materials containing single-domain magnetic particles in a non-magnetic matrix. The most straightforward approach would be a linear model [21], where the intrinsic susceptibility of the composites,  $\chi_{nc}$ , is simply the particle volume fraction,  $f$ , times the particle susceptibility

$$\chi_{nc} = f\chi_p. \quad (24)$$

This model is often used implicitly for ferromagnetic fluids or other dilute particle systems [34]. It seems readily adaptable to describe the susceptibility of a system of single-domain particles where the particle susceptibility is not limited to  $1/N$ , but the validity of the model has

not yet been systematically investigated for dense particle systems. In cases where inter-particle interactions prevail, composite susceptibility may deviate from linear.

Recently, Bjørk and Bahl [35] proposed a global demagnetisation factor that depends on particle volume fraction and on the demagnetisation factors of both spherical particles and sample shape. As stated by Bjørk and Bahl [35], this model should, however, not be applied to samples containing isolated single-domain particles. We agree with Bjørk and Bahl that their demagnetisation factor [35] should not be used for deriving the susceptibility of nanoparticle systems. We base this on our theoretical derivations in Sect. II B 1 showing that the particle susceptibility is not limited by the particle demagnetisation like for multi-domain particles and should be corrected for the sample shape, but not necessarily the particle shape.

Normile et al. [36] have used the demagnetization factor from Bahl and Bjørk [35], which includes a correction for both sample and particle shapes, to derive the intrinsic susceptibility of 8 nm maghemite particles in dense assemblies. However, they get large discrepancies in intrinsic susceptibilities (5 vs. 15) for similar particles in thin and thick disks configuration and similar volume fraction (50 vs 59 volume %). If their measured susceptibilities had only been corrected for the sample shape, then the intrinsic susceptibilities would have been more similar (e.g. 3.7 vs 4.3 for the case where the applied field is parallel to the disk plane). This supports that the demagnetization factor from Bahl and Bjørk [35] is not applicable to single-domain nanoparticle systems.

Hence, in order to derive  $\chi_{nc}$  from experimental measurements on nanocomposites, we apply the following procedure: for a specific sample (e.g. a thin disc of nanocomposite), the effective susceptibility is measured in a certain direction and the measurement is demagnetisation corrected for the sample shape only.

#### D. Nanocomposite losses

Hysteresis loops of superparamagnetic particles may open when high frequency fields are applied to the particles resulting in losses. At small applied fields the hysteresis losses can be calculated from the out-of-phase component of the susceptibility (Eqs. (18)-(23)). As the nanocomposite susceptibility varies with volume fraction of particles (Eq. (24)), so does the field  $H$  needed to obtain a certain magnetic flux in the material. Hence, for a given application with a required flux density, the loss will be larger for a low susceptibility material than for high susceptibility materials due to the need for larger applied field. Hence, the losses will increase with a decreasing volume fractions of particles when the nanocomposites generate equal magnetisation.

Table I lists calculated susceptibilities and losses at 2 MHz for composites of 30 volume %  $20\pm1$  nm FeNi particles with anisotropy axes oriented parallel, perpendic-

Table I: Calculated susceptibility and losses of nanocomposites containing 30 vol% spherical FeNi particles with 3 different easy axis arrangements. Calculations are based on  $\omega/(2\pi) = 2$  MHz, using Eqs. (18)-(23) with an applied field amplitude  $H$  such that 30 mT flux density is achieved in the composite,  $\tau_0 = 10$  ns,  $T = 298$  K, material parameters as in Fig. 3, and log-normal distributed particle diameters of  $20\pm1$  nm.

| Material and orientation | $\chi'_{\text{spm}}$ | $\chi''_{\text{spm}}$ | $H$ [A/m] | Power loss [mW/cm <sup>3</sup> ] |
|--------------------------|----------------------|-----------------------|-----------|----------------------------------|
| FeNi                     | 487                  | 11                    | 49        | 180                              |
| FeNi Random              | 209                  | 3.6                   | 114       | 330                              |
| FeNi $\perp$             | 70                   | 0.02                  | 341       | 20                               |

ularly and randomly wrt. the applied field. The losses are calculated assuming Eq. (24) and with an applied field amplitude  $H$  such that a flux density amplitude of 30 mT is achieved in the nanoparticle composites. From the calculated losses in table I, it is seen that for both the parallel and perpendicularly aligned cases, losses lower than 200 mW/cm<sup>3</sup> are possible. The aligned particles have lower losses at a given flux density than the random case due to lower applied field amplitude used to reach the desired flux density. Based on these calculations, the susceptibility and losses of perpendicularly and parallel aligned, spherical single-domain FeNi nanoparticles seem promising for micro-inductor applications.

## IV. EXPERIMENTAL VERIFICATION

In order to test our predictions on magnetic single-domain particles and verify that effective particle susceptibilities above  $1/N$  are possible, we prepared and investigated nanocomposites containing spherical, single-domain  $\gamma\text{-Fe}_2\text{O}_3$  (maghemite) particles in a polymer matrix. From Transmission Electron Microscopy (TEM) it was found that particle size was log-normal distributed with a mean diameter of 11 nm and a standard deviation of 3 nm, hereafter denoted as  $11\pm3$  nm. Small-angle neutron scattering (SANS) confirms near spherical particle shape and absence of aggregation in the polymer matrix.  $\gamma\text{-Fe}_2\text{O}_3$  was chosen for particle test material over metallic FeNi and FeCo despite maghemite's lower susceptibility due to maghemite's pure phase and no uncontrolled partial oxidation concerns in the synthesis. Detailed description and characterisation of the synthesised nanocomposites is presented elsewhere [Zambach et al., in preparation].

Nanocomposite samples for magnetic measurements were cast as discs with a thickness of 100-400  $\mu\text{m}$  and diameter of 6 mm. Hysteresis curves were measured in a vibrating sample magnetometer (VSM) with sample disc plane parallel to the applied field. All composite samples showed Langevin behaviour typical for superparamagnetic nanoparticles fitting with distributions similar to the TEM results. No detectable hysteresis was found

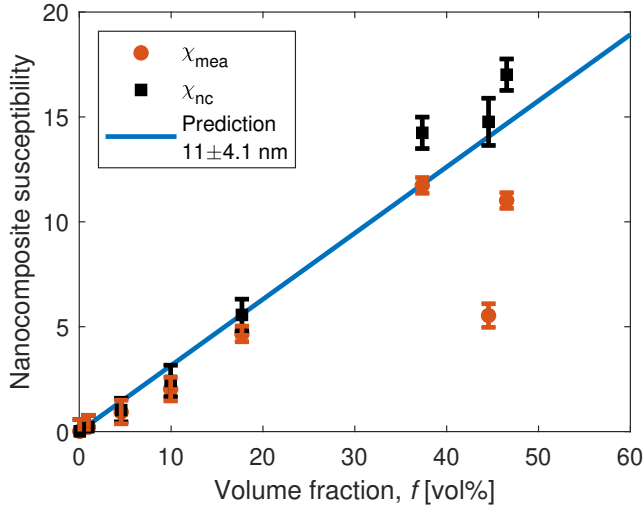


Figure 5: Measured susceptibility of nanocomposites containing randomly oriented  $11 \pm 3$  nm diameter  $\gamma\text{-Fe}_2\text{O}_3$  particles as function of volume fraction of particles together with theoretic prediction.  $\chi_{\text{mea}}$  is the measured nanocomposite susceptibility and  $\chi_{\text{nc}}$  is the measured susceptibility corrected for the sample shape according to [38]. Theoretic prediction based on Eq. (20), maghemite saturation magnetisation  $M_s = 303$  kA/m, log-normal distributed mean particle diameter of  $11 \pm 4.1$  nm,  $T = 298$  K, and Eq. (24).

with coercive fields below  $4 \pm 8$  A/m at 298 K. Magnetic particle content was calculated by comparison with particle saturation magnetisation found from liquid samples for which iron content was measured by inductively coupled plasma mass spectrometry (ICP-MS) [37]. Volume fraction of particles was then calculated by use of measured matrix density of 1 g/cm<sup>3</sup> and maghemite density of 4.88 g/cm<sup>3</sup>.

Figure 5 shows resulting nanocomposite susceptibilities found from magnetisation measurements,  $\chi_{\text{mea}}$  (red) as measured, and  $\chi_{\text{nc}}$  (black) with demagnetisation correction for macroscopic sample shape (disk /flat cylinder). The used sample shape demagnetisation factors are calculated according to Ref. [38]. The relatively smaller  $\chi_{\text{mea}}$  of the sample with 44 vol% is due to its thicker disk size, and, when demagnetisation corrected for the sample shape, the nanocomposite material follows the linear trend for  $\chi_{\text{nc}}$ .

The theoretic prediction, shown as full line in Fig. 5, is based on Eqs. (20) and (24), log-normally distributed maghemite particles with a mean diameter of  $11 \pm 4.1$  nm, and  $M_s = 303 \pm 9$  kA/m. We note that the sample shape demagnetisation corrected susceptibilities  $\chi_{\text{nc}}$  are in agreement with our predictions, despite a slightly larger log-normal distribution width than derived from TEM (4.1 nm vs 3 nm), but this variation is within the experimental uncertainty of the TEM data.

The measured composite susceptibility, which is significantly larger than 3 and in agreement with our theoret-

ical predictions, clearly exemplifies that the superparamagnetic, single-domain particles are not limited by demagnetisation effects to  $1/N$  due to particle shape. We further note that the synthesised nanocomposites have higher susceptibility than to our knowledge reported in literature for well-dispersed single-domain particles.

Noticeably, the high susceptibilities ( $\gg 3$ ) (cf. Fig. 5) also expose experimentally that the demagnetisation factor in Refs. [35, 36], which correct for both particle shape and sample shape (cf. Sect. III C), is not applicable to nanoparticle systems. First of all, the measured susceptibilities,  $\chi_{\text{mea}}$ , of 11.0 - 11.7 (Fig. 5), are simply too high to be explained by the demagnetization factor in Refs. [35, 36].  $\chi_{\text{mea}}$  could maximally be 5.6 for 46 vol% of spherical nanoparticles, if using the demagnetisation factor in Refs. [35, 36]. Moreover, if the here measured susceptibilities of 4.7-11.7 for the 17-46 vol% samples (Fig. 5) are demagnetisation corrected for both particle shape and sample shape, as in [35, 36], then meaningless negative intrinsic susceptibilities,  $\chi_{\text{nc}}$ , of -5.1 to -9.4, are obtained, emphasising the demagnetisation factor given in Refs. [35, 36] is not applicable to systems of superparamagnetic single-domain nanoparticles. Rather,  $\chi_{\text{mea}}$  should be corrected for sample shape, but not spherical particle shape.

While this nanocomposite susceptibility (Fig. 5), however, is not above the usable limit of 20 for micro-inductors, our results show that superparamagnetic particles are not limited by demagnetisation, and that nanocomposite susceptibility can follow a linear trend wrt. volume fraction; this opens up for new ways to think material designs for micro-inductors. With optimised particle parameters (high saturation magnetisation and low anisotropy) susceptibilities above 100 are theoretically possible, potentially with lower losses than today's state-of-the-art ferrite materials.

In our test samples containing up to 46 vol%  $11 \pm 4.1$  nm  $\gamma\text{-Fe}_2\text{O}_3$  particles, we do not observe clear signs of inter-particle interactions, but in general influences of inter-particle interactions are a potential concern for the design of dense nanoparticle composites. Inter-particle interactions can lead to deviations from the calculated linear non-interacting susceptibility in Fig. 5. In literature interactions have been predicted to either increase or decrease particle susceptibility [6, 39-41]. We estimate the dipolar interaction between particle pairs in our system (1-46 vol%  $11 \pm 4.1$  nm  $\gamma\text{-Fe}_2\text{O}_3$ ) to be on the scale of 50-500 K, using  $\mu_0 m^2 / (4\pi r_{\text{cc}}^3 k_B)$ , where  $r_{\text{cc}}$  is the mean center-center distance of the particles. This estimate does not take into account the fluctuating nature of the particle magnetisation and that one particle has several neighbours which may lead to increased/decreased interaction fields. When comparing to the anisotropy barrier ( $KV/k_B$ ) which is in the range of 1200 K, the found interaction energy scale for our system may be insignificant. As the dipolar interactions scales with  $m^2/r_{\text{cc}}^3$  it could likely be more pronounced in systems with larger particles with larger  $M_s$  such as 20 nm FeNi particles. Interac-

tions may also influence the effective anisotropy, and thus change the frequency dependence and measured losses. The influence of inter-particle interactions is indeed a large topic that needs further investigations when considering nanoparticle composites for e.g. micro-inductor core materials.

## V. CONCLUSIONS

Our theoretical derivations show that effective single-domain particle susceptibility is not limited by demagnetisation, and for a given material, (near-)spherical particles will have the largest susceptibility. Spherical particles with small magnetic anisotropy and high saturation magnetisation, like FeNi, allow for particle susceptibilities higher than 700 (Figs. 3 and 4). Calculations further show that alignment of easy axis parallel to the applied field can increase composite susceptibility, resulting in lower power losses compared to the random orientation case for the same magnetic flux density (Table I). More-

over, the same particles aligned with the easy-axis perpendicular to the applied field will have lower susceptibility, while having reduced power losses and flat susceptibility up to the high MHz range. We have supported our theoretical derivations and predictions on the susceptibility of non-interacting particles with experimental validation. The model remains applicable for non-interacting multi-particle nanocomposite susceptibility with a linear dependence on particle volume fraction. A nanocomposite susceptibility around 17 was achieved for spherical superparamagnetic particles of  $\gamma$ -Fe<sub>2</sub>O<sub>3</sub>, clearly demonstrating that the conventional demagnetisation limit does not apply.

## ACKNOWLEDGMENTS

The authors thank Ron B. Goldfarb for providing helpful feedback to a previous version of this manuscript and the Independent Research Fund Denmark for financial support (project HiFMag, grant number 9041-00231A).

---

- [1] R. Yawger, Psma power technology roadmap [psma corner], Ieee Power Electronics Magazine **9**, 10 (2022).
- [2] M. Araghchini, J. Chen, V. Doan-Nguyen, D. V. Harburg, D. Jin, J. Kim, M. S. Kim, S. Lim, B. Lu, D. Piedra, J. Qiu, J. Ranson, M. Sun, X. Yu, H. Yun, M. G. Allen, J. A. Alamo, G. Desgroseilliers, F. Herrault, J. H. Lang, C. G. Levey, C. B. Murray, D. Otten, T. Palacios, D. J. Perreault, and C. R. Sullivan, A technology overview of the powerchip development program, Ieee Transactions on Power Electronics **28**, 4182 (2013).
- [3] TDK, Tdk electronics - ferrites and accessories - siferrit material pc200, <https://www.tdk-electronics.tdk.com/download/2111340/11693683fbf07f86ca883884ffb3ddcc/pdf-pc200.pdf> **SIFERRIT material PC200 - Datasheet, accessed dec. 1, 2022** (2017).
- [4] M. Petrecca, M. Albino, I. G. Tredici, U. Anselmi-Tamburini, M. Passaponti, A. Caneschi, and C. Sangregorio, High density nanostructured soft ferrites prepared by high pressure field assisted sintering technique, Journal of Nanoscience and Nanotechnology **19**, 4974 (2019).
- [5] W. G. Hurley, T. Merkin, and M. Duffy, The performance factor for magnetic materials revisited: The effect of core losses on the selection of core size in transformers, Ieee Power Electronics Magazine **5**, 26 (2018).
- [6] M. Kin, H. Kura, and T. Ogawa, Core loss and magnetic susceptibility of superparamagnetic fe nanoparticle assembly, Aip Advances **6**, 125013 (2016).
- [7] C. Garnero, M. Lepesant, C. Garcia-Marcelot, Y. Shin, C. Meny, P. Farger, B. Warot-Fonrose, R. Arenal, G. Viau, K. Soulantica, P. Fau, P. Poveda, L. M. Lacroix, and B. Chaudret, Chemical ordering in bimetallic fe-co nanoparticles: From a direct chemical synthesis to application as efficient high-frequency magnetic material, Nano Letters **19**, 1379 (2019).
- [8] D. Hasegawa, H. Yang, T. Ogawa, and M. Takahashi, Challenge of ultra high frequency limit of permeability for magnetic nanoparticle assembly with organic polymer-application of superparamagnetism, Journal of Magnetism and Magnetic Materials **321**, 746 (2009).
- [9] M. P. Rowe, S. Sullivan, R. D. Desautels, E. Skoropata, and J. Van Lierop, Rational selection of superparamagnetic iron oxide/silica nanoparticles to create nanocomposite inductors, Journal of Materials Chemistry C **3**, 9789 (2015).
- [10] H. Yun, X. Liu, T. Paik, D. Palanisamy, J. Kim, W. D. Vogel, A. J. Viescas, J. Chen, G. C. Papaefthymiou, J. M. Kikkawa, M. G. Allen, and C. B. Murray, Size- and composition-dependent radio frequency magnetic permeability of iron oxide nanocrystals, Acs Nano **8**, 12323 (2014).
- [11] H. Yun, J. Kim, T. Paik, L. Meng, P. S. Jo, J. M. Kikkawa, C. R. Kagan, M. G. Allen, and C. B. Murray, Alternate current magnetic property characterization of nonstoichiometric zinc ferrite nanocrystals for inductor fabrication via a solution based process, Journal of Applied Physics **119**, 113901 (2016).
- [12] K. Yatsugi, T. Ishizaki, K. Akedo, and M. Yamauchi, Composition-controlled synthesis of solid-solution fe-ni nanoalloys and their application in screen-printed magnetic films, Journal of Nanoparticle Research **21**, 60 (2019).
- [13] H. Kura, T. Ogawa, R. Tate, K. Hata, and M. Takahashi, Size effect of fe nanoparticles on the high-frequency dynamics of highly dense self-organized assemblies, Journal of Applied Physics **111**, 07B517 (2012).
- [14] N. A. Usov and J. M. Barandiarán, Magnetic nanoparticles with combined anisotropy, Journal of Applied Physics **112**, 053915 (2012).
- [15] E. Stoner and E. Wohlfarth, A mechanism of magnetic hysteresis in heterogeneous alloys, Philosophical

Transactions of the Royal Society of London Series A- mathematical and Physical Sciences **240**, 599 (1948).

[16] P. Svedlindh, T. Jonsson, and J. L. García-Palacios, Intra-potential-well contribution to the ac susceptibility of a noninteracting nano-sized magnetic particle system, Journal of Magnetism and Magnetic Materials **169**, 323 (1997).

[17] N. A. Usov and S. E. Peschany, Theoretical hysteresis loops for single-domain particles with cubic anisotropy, Journal of Magnetism and Magnetic Materials **174**, 247 (1997).

[18] I. Joffe and R. Heuberger, Hysteresis properties of distributions of cubic single-domain ferromagnetic particles, Philosophical Magazine **29**, 1051 (1974).

[19] M. Walker, P. Mayo, K. OGrady, S. Charles, and R. Chantrell, The magnetic-properties of single-domain particles with cubic anisotropy .1. hysteresis loops, Journal of Physics-condensed Matter **5**, 2779 (1993).

[20] F. Ludwig, C. Balceris, and C. Johansson, The anisotropy of the ac susceptibility of immobilized magnetic nanoparticles-the influence of intra-potential-well contribution on the ac susceptibility spectrum, Ieee Transactions on Magnetics **53**, 7894242 (2017).

[21] J. Carrey, B. Mehdaoui, and M. Respaud, Erratum: Simple models for dynamic hysteresis loop calculations of magnetic single-domain nanoparticles: Application to magnetic hyperthermia optimization (journal of applied physics (2011) 109 (083921)), Journal of Applied Physics **110**, 039902 (2011).

[22] Y. L. Raikher and M. I. Shliomis, Dispersion theory of the magnetic susceptibility of small ferromagnetic particles, Zhurnal Eksperimental'noi I Teoreticheskoi Fiziki **67**, 1060 (1974).

[23] M. Shliomis and V. Stepanov, Frequency-dependence and long-time relaxation of the susceptibility of the magnetic fluids, Journal of Magnetism and Magnetic Materials **122**, 176 (1993).

[24] J. Fock, M. F. Hansen, C. Frandsen, and S. Mørup, On the interpretation of mössbauer spectra of magnetic nanoparticles, Journal of Magnetism and Magnetic Materials **445**, 11 (2018).

[25] I. EISENSTEIN and A. AHARONI, High-order superparamagnetic relaxation-times, Physica B and C **86**, 1429 (1977).

[26] D. A. Smith and F. A. De Rozario, A classical theory of superparamagnetic relaxation, Journal of Magnetism and Magnetic Materials **3**, 219 (1976).

[27] Y. P. Kalmykov, Longitudinal dynamic susceptibility and relaxation time of superparamagnetic particles with cubic anisotropy: Effect of a biasing magnetic field, Physical Review B (condensed Matter) **61**, 6205 (2000).

[28] Y. P. Kalmykov and S. V. Titov, Nonlinear response of superparamagnetic particles with cubic anisotropy to a sudden change in the applied strong static magnetic field, Physics of the Solid State **44**, 2276 (2002).

[29] P. C. Rivas Rojas, P. Tancredi, C. L. Londoño-Calderón, O. Moscoso Londoño, and L. M. Socolovsky, Comparison of the anisotropy energy obtained from temperature dependent ac and dc magnetometry in iron oxide nanoparticles (ionps) with controlled dipolar interactions, Journal of Magnetism and Magnetic Materials **547**, 168790 (2022).

[30] M. Bohra, S. V. Battula, V. Alman, A. Annadi, and V. Singh, Design of various ni-cr nanostructures and deducing their magnetic anisotropy, Applied Nanoscience (switzerland) , 1 (2021).

[31] F. Bødker, S. Mørup, and S. Linderoth, Surface effects in metallic iron nanoparticles, Physical Review Letters **72**, 282 (1994).

[32] L. M. Lacroix, R. B. Malaki, J. Carrey, S. Lachaize, M. Respaud, G. F. Goya, and B. Chaudret, Magnetic hyperthermia in single-domain monodisperse feco nanoparticles: Evidences for stoner-wohlfarth behavior and large losses, Journal of Applied Physics **105**, 023911 (2009).

[33] K. Kumari, A. Kumar, J. E. Lee, and B. H. Koo, Investigating the origin of exchange bias effect in ferromagnetic feni nanoparticles prepared via controlled synthesis, Applied Nanoscience (switzerland) , 1 (2021).

[34] K. Bai, J. Casara, A. Nair-Kanneganti, A. Wahl, F. Carle, and E. Brown, Effective magnetic susceptibility of suspensions of ferromagnetic particles, Journal of Applied Physics **124**, 123901 (2018).

[35] R. Bjørk and C. R. Bahl, Demagnetization factor for a powder of randomly packed spherical particles, Applied Physics Letters **103**, 102403 (2013).

[36] P. S. Normile, M. S. Andersson, R. Mathieu, S. S. Lee, G. Singh, and J. A. De Toro, Demagnetization effects in dense nanoparticle assemblies, Applied Physics Letters **109**, 152404 (2016).

[37] R. Costo, D. Heinke, C. Grüttner, F. Westphal, M. P. Morales, S. Veintemillas-Verdaguer, and N. Gehrke, Improving the reliability of the iron concentration quantification for iron oxide nanoparticle suspensions: a two-institutions study, Analytical and Bioanalytical Chemistry **411**, 1895 (2019).

[38] M. Beleggia, M. De Graef, Y. T. Millev, D. A. Goode, and G. Rowlands, Demagnetization factors for elliptic cylinders, Journal of Physics D: Applied Physics **38**, 3333 (2005).

[39] E. A. Elfimova, A. O. Ivanov, and P. J. Camp, Static magnetization of immobilized, weakly interacting, superparamagnetic nanoparticles, Nanoscale **11**, 21834 (2019).

[40] R. W. Chantrell, N. Walmsley, J. Gore, and M. Maylin, Calculations of the susceptibility of interacting superparamagnetic particles, Physical Review B - Condensed Matter and Materials Physics **63**, 024410/1 (2001).

[41] N. A. Usov and O. N. Serebryakova, Equilibrium properties of assembly of interacting superparamagnetic nanoparticles, Scientific Reports **10**, 13677 (2020).